Journal of Applied Physics ARTICLE scitation.org/journal/jap

Optical excitation density dependence of spin dynamics in bulk cubic GaN

Cite as: J. Appl. Phys. **126**, 153901 (2019); doi: 10.1063/1.5123914
Submitted: 9 August 2019 · Accepted: 1 October 2019 ·
Published Online: 15 October 2019

J. H. Buß,[1] T. Schupp,[2] D. J. As,[2] D. Hägele,[1] and J. Rudolph[1,a)]

AFFILIATIONS

[1]Experimental Physics VI (AG), Faculty of Physics and Astronomy, Ruhr University Bochum, 44801 Bochum, Germany
[2]Department Physik, Universität Paderborn, Warburger Str. 100, 33098 Paderborn, Germany

[a)]**Electronic mail:** joerg.rudolph@ruhr-uni-bochum.de

ABSTRACT

The influence of the optical excitation density on the electron spin dynamics is experimentally investigated in bulk cubic GaN by time-resolved magneto-optical Kerr-rotation spectroscopy. The nanosecond spin relaxation times in moderately *n*-doped *β*-GaN decrease with increasing excitation density, though the effective lifetimes of the optically excited carriers are almost two orders of magnitude shorter than the spin relaxation times. This counterintuitive finding is explained by the heating of the electron system due to the excitation process. The spin relaxation times in degenerately *n*-doped *β*-GaN are found to be independent of excitation density as the very high electron Fermi temperature completely dominates over carrier heating processes in this case.

I. INTRODUCTION

The electron spin dynamics in semiconductors depends in a complex way on numerous parameters, with both extrinsic quantities like temperature or magnetic field as well as intrinsic material properties like the crystal structure or strength of spin orbit coupling (SOC) influencing the spin dynamics.[1] Another key parameter for electron spin relaxation is in general the electron density, which can be tuned via the doping level.[2–4] The density of photoexcited carriers can influence the spin dynamics in optical experiments in a similar way. The density as well as the excess energy of photoexcited electrons can be conveniently tuned in such experiments, thus opening an interesting access to the investigation of spin dynamics.

Experimentally, a decrease of the electron spin relaxation time for increasing optical excitation density has been found in *n*-type bulk GaAs[5–10] and GaSb,[11] while an increase of the spin relaxation time was found for low excitation densities in intrinsic GaAs.[7,12] Nonmonotonic density dependencies with maximum spin relaxation times at intermediate excitation densities were reported in bulk CdTe,[13–15] CdZnTe,[14] and InP.[16] Similarly, a nonmonotonic density dependence of the spin relaxation time was found at room-temperature in (001)GaAs quantum wells (QWs),[10] while increasing spin relaxation times for increasing density were found at 80 K.[17] In (110)GaAs QWs, either a nonmonotonic density dependence[18] or a decrease of the spin relaxation time for increasing density was reported at room temperature.[19]

A general theoretical description of the observed density dependencies is, however, lacking, as the experimental results were either left unexplained[5,6] or attributed to the dominance of either the Dyakonov-Perel (DP) spin relaxation mechanism,[7,12,13,15,16] the Elliott-Yafet mechanism,[13] or the Bir-Aronov-Pikus mechanim[9,10] or to possible hot-electron effects caused by the photoexcitation process.[11,20] Calculations based on a microscopic kinetic spin Bloch equation approach predict the overall dominance of the DP mechanism,[2,21,22] however, they completely neglect not only possible excitonic effects[23] but also the dynamics of the photoexcited electrons, e.g., by treating the density of photoexcited electrons as constant. This widely applied approximation[2,10,21,22,24,25] corresponds to an effective lifetime τ_ℓ^{eff} of the optically excited carriers which largely exceeds their spin relaxation time τ_s. The condition $\tau_\ell^{\mathrm{eff}} \gg \tau_s$ is, however, often not or only approximately fulfilled in the experiment[9,12–16] or not considered at all,[5–8,10,11] making the applicability of the mentioned approximations questionable. The investigation of the opposite situation, where spin lifetimes largely exceed the effective lifetimes of the optically created carriers, is, therefore, highly relevant for a deepened understanding of the influence of the optical excitation process on the observed spin dynamics. The metastable zincblende phase of GaN (*β*-GaN) is

ideally suited for such studies as it shows short effective carrier lifetimes[26,27] but long spin relaxation times in the nanoseconds range.[28]

Here, we experimentally investigate the optical excitation density dependence of the electron spin dynamics in bulk β-GaN by time-resolved Kerr-rotation (TRKR) measurements. We find decreasing spin relaxation times for increasing excitation density in moderately n-doped β-GaN, while the spin relaxation times in degenerately n-doped β-GaN are independent of the excitation density. These findings are explained by carrier heating effects, which no longer occur for the high Fermi temperatures at high doping levels.

II. SAMPLES AND EXPERIMENTAL SETUP

The β-GaN epilayers were grown by plasma-assisted molecular beam epitaxy.[29] A 580 nm-thick β-GaN layer was deposited on top of a 15–40 nm wide zincblende β-AlN barrier on a 3C-SiC substrate. Si n-type doping results in electron densities of 1×10^{17} cm^{-3} for sample C1, 1×10^{18} cm^{-3} for sample C2, and 1×10^{19} cm^{-3} for sample C3, respectively, for the top β-GaN layer.

Photoluminescence (PL) was excited by frequency-doubled femtosecond-pulses of a modelocked Ti:sapphire laser at an energy of 3.55 eV. The laser was focused to a spot with a diameter of 100 μm on the sample surface, and the emitted PL was spectrally and temporally resolved by a syncroscan streak camera setup. The sample was mounted in a cold-finger cryostat and kept at a temperature of $T = 80$ K.

Time-resolved Kerr-rotation measurements were performed using the frequency-doubled output of a wavelength-tunable modelocked Ti:sapphire laser, which was split into pump and probe beams. The pump beam was focused down to a spot with a diameter of 100 μm on the sample surface, where it excited a spin-polarized electron ensemble. The temporal evolution of the spin polarization was tracked via the Kerr-rotation of the linearly polarized probe pulse, which was temporally delayed with respect to the pump pulse via a mechanical delay line. A cascaded lock-in amplifier detection scheme with double modulation including polarization modulation of the pump pulse was used for sensitive detection.[30] The power of pump and probe beam was kept typically at a ratio of 10:1. The sample was mounted in a cold-finger cryostat and an external magnetic field B_{ext} was applied in the sample plane.

The density of photoexcited carriers n_{exc} was estimated via

$$n_{\mathrm{exc}} = (1 - R)[1 - \exp(\alpha d_s)]P_{\mathrm{exc}}/(A f_{\mathrm{rep}} \hbar\omega_{\mathrm{exc}} d_s), \qquad (1)$$

with R as the combined reflectivity of the cryostat window and the sample, α as the absorption coefficient, d_s as the epilayer thickness, P_{exc} as the average excitation power, $A = \pi R_{\mathrm{spot}}^2$ as the area of the pump spot, where R_{spot} is the spot radius, f_{rep} as the repetition frequency of the laser, and $\hbar\omega_{\mathrm{exc}}$ as the photon energy of the pump laser. A value of $\alpha = 1 \times 10^5$ cm^{-1} was used for the absorption coefficent at the pump energy.[31]

III. EXPERIMENTAL RESULTS AND DISCUSSION

In Sec. III A, we will first discuss the photoluminescence characteristics of the samples under investigation, before we turn to the electron spin dynamics as the central point of this work.

A. Photoluminescence

The time-integrated PL spectra of the lower doped samples C1 and C2 are characterized by three peaks [cf. Fig. 1(a)]. The dominating peak at 3.24 eV originates from the spectrally overlapping recombination of free and bound excitons.[26,32] Additional peaks at 3.15 eV and 3.06 eV correspond to a band-acceptor (e, A^0) transition and its LO-phonon replica, respectively.[32,33] The (e, A^0) transition becomes more pronounced with increasing excitation density. The corresponding PL transients of the excitonic peak show for all investigated excitation densities a biexponential decay. The effective decay times[34] of the fast and slow components $\tau_{\ell,\mathrm{f}}^{\mathrm{eff}} \approx 10$ ps and $\tau_{\ell,\mathrm{sl}}^{\mathrm{eff}} \approx 80$ ps, respectively, of the decay

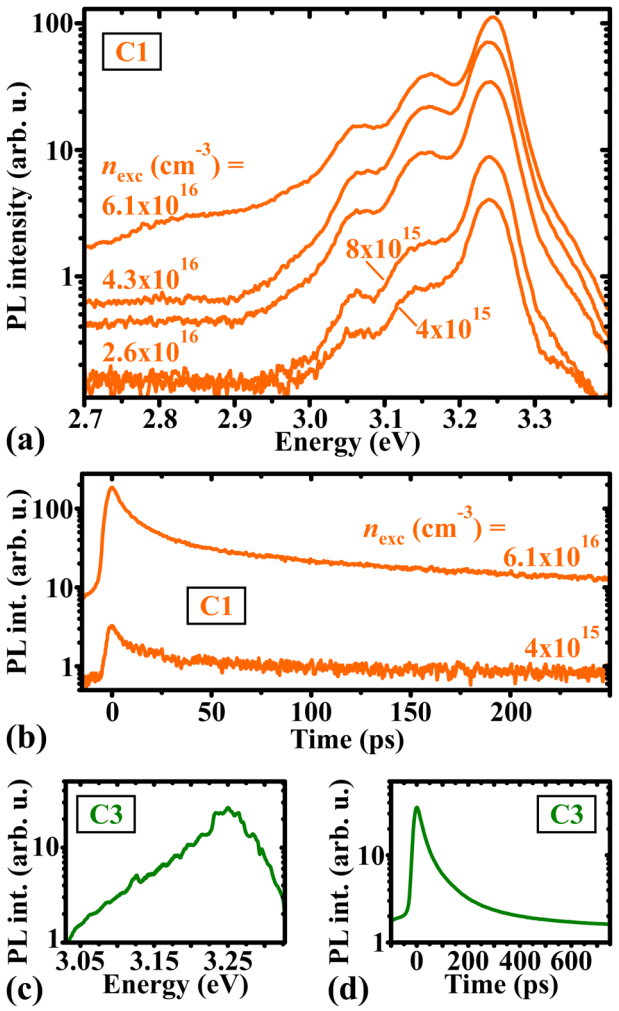

FIG. 1. (a) Time-integrated photoluminescence spectra and (b) photoluminescence transients at the energy of maximum photoluminescence emission for sample C1 for different excitation densities at a temperature of $T = 80$ K. (c) Time-integrated photoluminescence spectrum and (d) photoluminescence transient for sample C3 at an excitation density of 4×10^{16} cm^{-3}.

compare well with typical values from the literature.[26,27] While the PL of sample C2 (not shown) is very similar to the one of sample C1, the degenerately doped sample C3 shows an extremely broad and asymmetric PL spectrum [cf. Fig. 1(c)], as being typical for degenerately doped bulk semiconductors due to band-to-band transitions or recombination of free electrons with localized hole states.[29] The PL transient at the energy of maximum PL emission shows again a biexponential decay characterized by a fast component with $\tau^{\mathrm{eff}}_{\ell,\mathrm{f}} \approx 30$ ps and a slow component with $\tau^{\mathrm{eff}}_{\ell,\mathrm{sl}} \approx 140$ ps [cf. Fig. 1(d)].

B. Time-resolved Kerr-rotation

Typical TRKR transients are shown exemplarily for sample C1 at different excitation densities in Fig. 2, where the excitation energy $E_{\mathrm{exc}} = 3.27$ eV was set to the maximum Kerr-rotation signal. The oscillations of the TRKR signal are due to spin Larmor precession around the external magnetic field B_{ext} with the Larmor precession frequency

$$\omega_L = g\mu_B B_{\mathrm{ext}}/\hbar, \tag{2}$$

where g is the Landé g-factor. The temporal decay of the TRKR signal amplitude is caused by spin relaxation of photoexcited and resident electrons, which have acquired spin polarization from the photogenerated electrons, as well as by the decay of the initially excited carrier density. To account for the latter, an exponential decay fit of the form $[A_1\exp(-t/\tau_c) + A_2]\exp(-t/\tau_s)\cos[\omega_L(t - t_0)]$ to the TRKR transients was employed, where τ_s is the spin relaxation time, while τ_c is a free fit parameter for an effective carrier decay time.[35]

The Larmor precession frequency ω_L shows for all three samples a perfectly linear dependence on the external magnetic field following Eq. (2) [cf. Figs. 3(a) and 3(b)], thus demonstrating purely electronic spin dynamics without excitonic contributions on a nanosecond time scale.[36] The g-factor $g \approx 1.95$ obtained from the magnetic field dependence $\omega_L(B_{\mathrm{ext}})$ agrees with the literature value[37] and shows within the experimental error no dependence on the doping density, excitation density, or excitation energy, respectively, [cf. Fig. 3(c) and 3(d)] as a consequence of the combination of weak spin orbit coupling and large bandgap in β-GaN.[38,39]

In the remaining, we will discuss the electron spin relaxation as the main point of this work, starting with the dependence of spin relaxation on the excitation density as shown in Fig. 4. The two lower doped samples C1 and C2 show overall long spin relaxation times on the order of several nanoseconds [cf. Fig. 4(a)]. The spin relaxation times are hence almost two orders of magnitude longer than the effective carrier lifetimes $\tau^{\mathrm{eff}}_{\ell}$ as determined by time-resolved photoluminescence (see previous section). Still, the spin relaxation times decrease with increasing excitation density as can already be seen from the raw data shown in Fig. 2(b) on a semilogarithmic scale. The decrease is pronounced for sample C1 with the lowest doping level, while the density dependence starts to flatten out for the higher doped sample C2. The spin

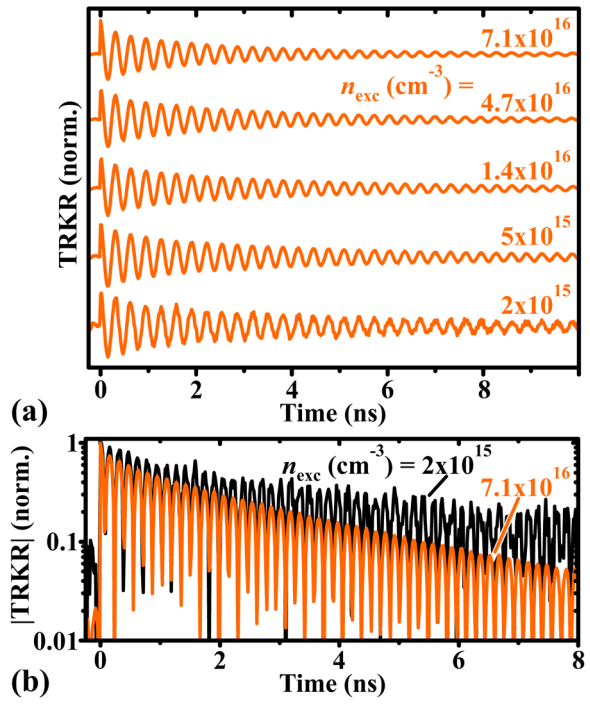

FIG. 2. (a) Time-resolved Kerr-rotation transients for sample C1 for different excitation densities at an excitation energy of $E_{\mathrm{exc}} = 3.27$ eV, a temperature of $T = 80$ K, and in an external magnetic field $B_{\mathrm{ext}} = 0.1$ T. (b) Absolute values of the TRKR transients of sample C1 for excitation densities of 2×10^{15} and 7.1×10^{16} cm^{-3}, respectively, on a semilog scale.

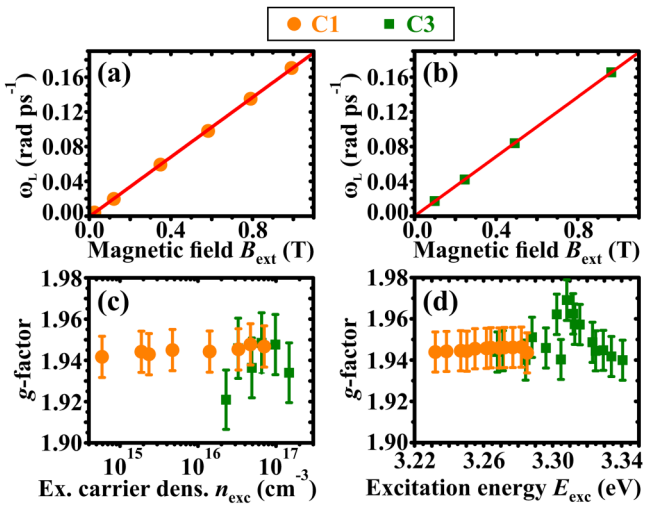

FIG. 3. Magnetic field dependence of the Larmor precession frequency ω_L for (a) sample C1 and (b) sample C3. The solid lines show linear fits to $\omega_L(B_{\mathrm{ext}})$ according to Eq. (2). (c) Excitation density dependence and (d) excitation energy dependence of the Landé g-factor for samples C1 (dot symbols) and C3 (square symbols).

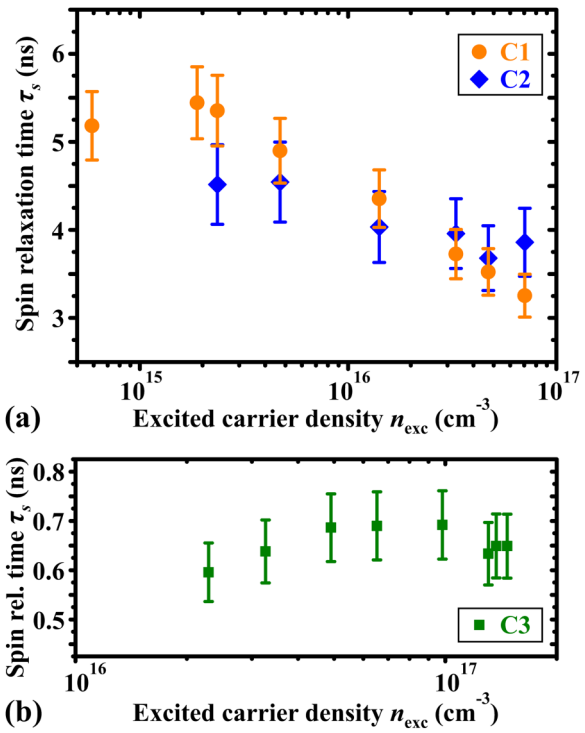

FIG. 4. Excitation density dependence of the spin relaxation time τ_s for (a) samples C1 and C2 at an excitation energy $E_{exc} = 3.27$ eV and (b) sample C3 at $E_{exc} = 3.29$ eV for a temperature of $T = 80$ K and an external magnetic field $B_{ext} = 0.1$ T.

relaxation times for the degenerately doped sample C3 are significantly shorter and independent of the excitation density [cf. Fig. 4(b)].

To understand the observed excitation density dependence, we will discuss the relevant spin relaxation mechanisms, which contribute in general to spin relaxation in bulk semiconductors and could lead to the observed excitation density dependence. The Elliott-Yafet[40,41] and the Bir-Aronov-Pikus mechanism[42] have been invoked to explain density dependent spin relaxation in CdTe[13] and GaAs,[9,10] respectively, they are, however, ineffective in n-type β-GaN.[28] We note that even the initially optically created hole population will not lead to a significant contribution of the Bir-Aronov-Pikus mechanism on a nanosecond time scale due to the short effective carrier lifetimes and subpicosecond excitonic spin relaxation in β-GaN.[43] The Elliott-Yafet and the Bir-Aronov-Pikus mechanisms will, therefore, not be considered further in the following. Instead, spin relaxation is dominated by the combined action of DP relaxation of delocalized electrons and hyperfine-interaction mediated spin relaxation of localized electrons.[28,44,45] Efficient spin exchange scattering leads to a single common spin relaxation rate

$$\gamma_s = f_{\mathrm{loc}}\gamma_s^{\mathrm{loc}} + (1 - f_{\mathrm{loc}})\gamma_s^{\mathrm{deloc}} \tag{3}$$

for both systems, where the contributions γ_s^{loc} from localized and $\gamma_s^{\mathrm{deloc}}$ from delocalized electrons are weighted by the degree of localization $f_{\mathrm{loc}} = n_{\mathrm{loc}}/n_{\mathrm{total}}$, with n_{loc} as the density of localized electrons and n_{total} as the total electron density.[30,46]

Spin relaxation of localized electrons is typically driven by hyperfine-interaction with the large number of lattice nuclei in the electrons' localization volume. The hyperfine interaction can be described as an effective nuclear magnetic field acting on the electron spins.[46] The corresponding spin relaxation rate follows for completely isolated electrons as

$$\gamma_s^{\mathrm{loc}} = \frac{1}{\hbar}\sqrt{\frac{2\sum_j I_j(I_j+1)A_j^2 y_j}{3N_L}}, \tag{4}$$

where y_j is the abundance, A_j is the hyperfine constant, I_j is the nuclear spin of isotope j of the lattice atoms, and N_L is the number of effectively interacting nuclei. While this hyperfine-interaction induced spin relaxation is independent of the electron density, its contribution to the total spin relaxation rate can in general depend on the electron density via the degree of localization [cf. Eq. (3)]. A significant influence of the optically excited carriers on the degree of localization is, however, not expected here for the nanoseconds time scale of spin relaxation as the effective carrier lifetimes τ_ℓ^{eff} are much shorter.

Instead, the observed excitation density dependence can be explained by Dyakonov-Perel relaxation as we will discuss in the following. DP spin relaxation of delocalized electrons is driven by an intrinsic conduction band spin splitting caused by spin orbit coupling.[47] This spin splitting can be interpreted as an effective magnetic field $\mathbf{\Omega}(\mathbf{k})$, which depends on the electron's wavevector $\mathbf{k}$ and forces the electron's spin to precess. Momentum scattering changes the electron's wavevector randomly, leading to spin dephasing for an electron ensemble. The corresponding SOC Hamiltonian

$$H_{\mathrm{soc}} = \frac{\hbar}{2}\mathbf{\Omega}(\mathbf{k})\cdot\boldsymbol{\sigma}, \tag{5}$$

with $\boldsymbol{\sigma}$ as the vector of Pauli spin matrices describes the conduction band spin splitting, from which the tensor of spin relaxation rates

$$\gamma_{s,ij}^{\mathrm{DP}} = \frac{1}{2}\left(\delta_{ij}\langle\mathbf{\Omega}^2\rangle - \langle\Omega_i\rangle\langle\Omega_j\rangle\right)\tau_p \equiv \langle\Omega_{\mathrm{eff}}^2\rangle\tau_p, \tag{6}$$

with $i, j = x, y, z$ follows in a basic approach,[48] where $\langle\cdots\rangle$ denotes the average over the electron distribution. Consequently, changes in the electron density influence the spin relaxation rate via the effective magnetic field average $\langle\Omega_{\mathrm{eff}}^2\rangle$ and via the effective momentum scattering time τ_p, which depends, in general, in a complex way on the electron density. The effective magnetic field $\mathbf{\Omega}(\mathbf{k})$ is due to the cubic k^3-Dresselhaus term[49]

$$\mathbf{\Omega}(\mathbf{k}) = \frac{2\gamma_e}{\hbar}\begin{pmatrix} k_x(k_y^2 - k_z^2) \\ k_y(k_z^2 - k_x^2) \\ k_z(k_x^2 - k_y^2) \end{pmatrix}, \tag{7}$$

in bulk β-GaN, where γ_e is the spin-splitting constant. For nondegenerate electrons, a spin relaxation rate

$$\gamma_{s,\mathrm{nd}}^{\mathrm{DP}} = \frac{16m^*3\gamma_e(k_BT)^3}{\hbar^8}\tau_p^{\mathrm{eff}} \tag{8}$$

follows from Eq. (6) for carrying out the average, assuming an isotropic Boltzmann distribution for the electron momentum distribution. The effective momentum scattering time τ_p^{eff} can be refined to include the individual efficiencies and energy dependencies of different momentum scattering mechanisms.[28,50] We note that the comparatively small spin-splitting constant and hence weak DP spin relaxation lead to the generally observed long spin relaxation times in β-GaN.[28,44,51,52]

In previous works, the excitation density dependence of spin relaxation has been explained via the DP mechanism by treating the optically excited electron density n_{exc} as temporally constant and by adding n_{exc} to the background electron density introduced by doping.[7,21,22] In close analogy to the doping density dependence of spin relaxation,[2,4,53,54] a nonmonotonic excitation density dependence has been predicted.[21,22] The nonmonotonic behavior results from different electron density dependencies of the effective magnetic field average $\langle\Omega_{\mathrm{eff}}^2\rangle$ and the effective momentum scattering time τ_p in the nondegenerate and the degenerate regime, respectively. This explanation can, however, not be directly transferred to the case studied here, as the optically excited carriers decay much faster than the spin polarization. Instead, not only the mere density of optically excited electrons has to be considered here but also their excess energy. The excess energy of photoexcited electrons is distributed among the whole electron system by carrier-carrier Coulomb scattering rapidly after the pulsed excitation. After this very fast initial thermalization, the electron system can be described by a thermal distribution with an electron temperature T_e, which can significantly exceed the lattice temperature T_L.[55,56] A higher electron temperature T_e leads to faster DP spin relaxation due to the occupation of higher k-states and a corresponding increase of the effective magnetic field average $\langle\Omega_{\mathrm{eff}}^2\rangle$ [cf. Eq. (6)]. Increasing optical excitation densities lead to an increasing electron temperature and consequently faster DP spin relaxation with decreasing spin relaxation times, just like observed here for the lowest doped sample C1. Estimating[57] a spin relaxation time of $\tau_s^{\mathrm{loc}} = 2.1$ ns for localized electrons according to Eq. (4) and of $\tau_s^{\mathrm{DP}} \approx 160$ ns for delocalized electrons at $T = 80$ K following Eq. (6) and the approach of Ref. 28,[58] we find a good agreement of the estimated total spin relaxation time $\tau_s^{\mathrm{est}} = 5.5$ ns with the experimentally observed spin relaxation time at low excitation densities for $f_{\mathrm{loc}} = 0.37$. Keeping τ_s^{loc} and f_{loc} fixed, the experimentally observed decrease of the spin relaxation time to $\tau_s = 3.5$ ns for high excitation density requires then a reasonable increase of the effective temperature for DP relaxation in Eq. (6) to $T_e = 195$ K.

The weak excitation density dependence for the higher doped sample C2 and the essentially constant spin relaxation times for the degenerately doped sample C3 are immediately understood from estimates of the electron Fermi temperature $T_F = E_F/k_B$ for these samples. Fermi temperatures of 282 and 1310 K follow for sample C2 and C3, respectively, using the Fermi energy $E_F = (3\pi^2)^{2/3}\hbar^2 n_D^{2/3}/2m^*$, with n_D as the electron density introduced by doping. As the Fermi temperature of the degenerately doped sample C3 strongly exceeds the lattice temperature, no further heating effect due to the optically excited electrons is expected, while for sample C2 with $T_F \gtrsim T_L$ a small heating effect is still possible. We note that hot-electron effects on spin relaxation have been mentioned in Ref. 11 and that the important role of the electron temperature for DP relaxation has been shown theoretically in Ref. 20.

After the fast initial thermalization, the electron temperature T_e approaches the lattice temperature T_L on longer time scales by energy relaxation. This energy relaxation process can be described in a basic approach by expressions for the average energy loss rates $\langle dE_c/dt\rangle$. The average excess energy loss rates per electron via one electron–one phonon interactions are given for conduction band electrons by[59]

$$\left\langle\frac{dE_c}{dt}\right\rangle_{lo} = -(2m^*)^{1/2}(\hbar\omega_{LO})^{3/2}\left(\frac{q}{\hbar}\right)^2\frac{\varepsilon_\infty^{-1}-\varepsilon^{-1}}{4\pi\varepsilon_0} \times\left[\exp\left(-\frac{\hbar\omega_{LO}}{k_BT_e}\right)-\exp\left(-\frac{\hbar\omega_{LO}}{k_BT_L}\right)\right] \tag{9}$$

for scattering by polar optical phonons,

$$\left\langle\frac{dE_c}{dt}\right\rangle_{pe} = -\frac{64\pi^{1/2}q^2e_{14}^2m^*3/2a(k_BT_e)^{1/2}}{2^{1/2}\hbar^2(4\pi\varepsilon_0)^2\varepsilon^2\rho}\frac{T_e-T_L}{T_e} \tag{10}$$

for piezoelectric scattering, and

$$\left\langle\frac{dE_c}{dt}\right\rangle_{dp} = -\frac{2^{1/2}8E_1^2m^*5/2(k_BT_e)^{3/2}}{\pi^{3/2}\hbar^4\rho}\frac{T_e-T_L}{T_e} \tag{11}$$

for deformation potential scattering. The emission of LO phonons is the dominating energy relaxation mechanism for a lattice temperature of $T_L = 80$ K as can be seen from Fig. 5(a), where the theoretical energy loss rates are plotted as a function of the electron temperature T_e using the material parameters of Table I and $a = 0.4$ as a dimensionless parameter. The corresponding cooling dynamics $T_e(t)$ follows from the energy loss equation

$$\frac{dT_e(t)}{dt} = \frac{2}{3k_B}\sum_{i=lo,pe,dp}\left\langle\frac{dE_c(T_e)}{dt}\right\rangle_i \tag{12}$$

and is shown in Fig. 5(b) for different initial electron temperatures T_e^{initial} resulting from the optical excitation. The electron temperature is hence predicted to reach the lattice temperature after about 100 ps within the simple model of carrier cooling sketched above. This time scale would be too short to explain the observed influence of the optical excitation density on the spin dynamics on a nanosecond time scale. The above description of electron cooling, however, completely neglects hot-phonon effects, which can strongly slow down the cooling process of the electrons.[60,61]

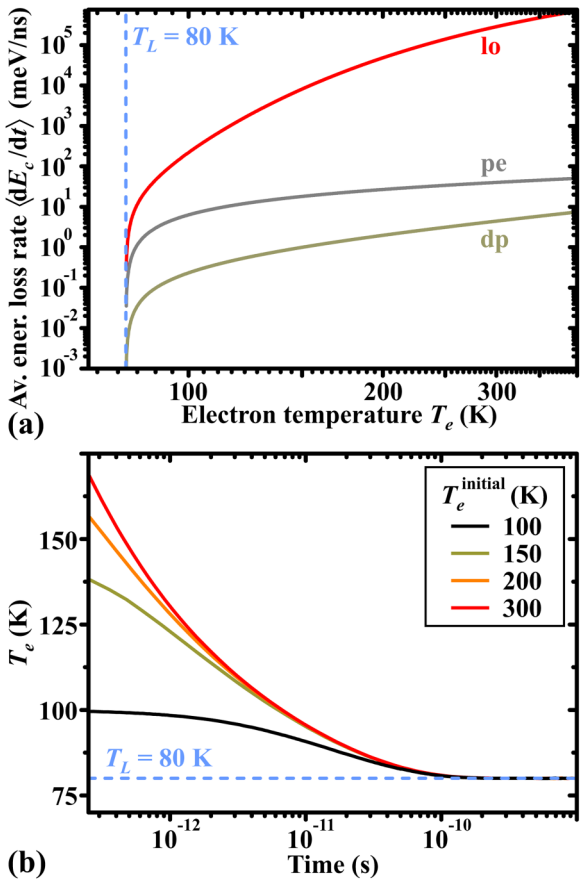

FIG. 5. (a) Theoretical average energy loss rates per electron as a function of the electron temperature T_e for scattering by polar optical phonons (lo), piezoelectric scattering (pe), and deformation potential scattering (dp) for different initial electron temperatures. (b) Electron cooling dynamics calculated within a simple one electron–one phonon interaction model neglecting hot-phonon effects. Note the semilog scale.

TABLE I. Material parameter for β-GaN.

	Symbol	Value	Reference
Effective electron mass	m^*	0.15 m_0	62
LO phonon frequency	$\tilde{\nu}_{LO}$	740 cm^{-1}	63
Static dielectric constant	ε	9.5 ε_0	64
High-frequency dielectric constant	ε_∞	5.35 ε_0	64
Piezoelectric constant	e_{14}	0.50 C/m^2	65
Mass density	ρ	6.15 g/cm^3	66
Deformation potential	E_1	2.77 eV	67
Thermal diffusivity	D	0.43 cm^2s^{-1}	66

The importance of hot-electron effects is further supported by the excitation energy dependent measurements of spin relaxation shown in Fig. 6. An increase of the excitation energyE_{exc} leads to decreasing spin relaxation times for sample C1 [cf. Fig. 6(a)], which can be readily understood from stronger heating for increasing electron excess energy corresponding to increasing excitation energy,[55] where the detailed excitation energy dependence of the electron temperature can, in general, be intricate.[68] The spin relaxation time in the degenerately doped sample C3 shows in contrast no dependence on the excitation energy [see Fig. 6(b)] as a consequence of the sample's high Fermi temperature $T_F \gg T_L$ (see above), which completely governs the temperature scale for this sample.

We note that the results of an analysis of the PL lineshape of the (e, A^0) transition (cf. Sec. III A) for different excitation densities also underline the importance of hot-electron effects. An effective temperature T_e^{PL} of the electron system can be extracted from the high-energy wing of the (e, A^0) transition by a fit of the form[69]

$$I_{(e,A^0)} \propto \sqrt{\hbar\omega - E_g + E_A}\,\exp\left(-\frac{\hbar\omega - E_g + E_A}{k_B T_e^{PL}}\right), \qquad (13)$$

with $\hbar\omega$ as the photon energy, E_g as the bandgap energy, and E_A as the effective acceptor binding energy. T_e^{PL} shows a pronounced increase with increasing excitation density for sample C1 (not shown) as a consequence of carrier heating.

Finally, a classical estimate of the time required for thermal equilibration of the thin, locally heated β-GaN epilayer with the

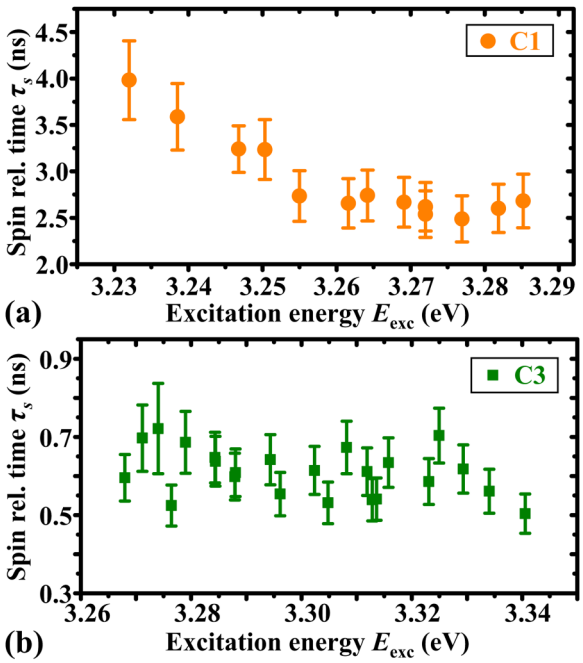

FIG. 6. Excitation energy dependence of the spin relaxation time τ_s in β-GaN for (a) sample C1 and (b) sample C3 at a temperature of $T = 80$ K.

underlying substrate by vertical heat diffusion is also compatible with the above interpretation. An equilibration time $\tau_{\mathrm{diff}}^{\mathrm{heat}} = 2d_s^2/D$ is estimated from the classical heat diffusion equation $\partial T/\partial t = D\Delta T$ with the substrate acting as a heat sink. The equilibration time $\tau_{\mathrm{diff}}^{\mathrm{heat}} \approx 15$ ns following for a thermal diffusivity of $D = 0.43\ \mathrm{cm}^2\ \mathrm{s}^{-1}$ (Ref. 66) does clearly not contradict the above interpretation.

IV. SUMMARY

To summarize, we have experimentally investigated the optical excitation density dependence of the electron carrier and spin dynamics in bulk β-GaN. We find a pronounced decrease of the spin relaxation time for increasing excitation density in moderately n-doped β-GaN, though the effective lifetime of the optically excited carriers is almost two orders of magnitude shorter than the nanosecond spin relaxation times. This surprising result is explained by the important role of hot-electron effects due to the optical excitation process. The electron spin dynamics is then determined by an effective electron temperature, which can largely exceed the lattice temperature. The excitation density dependence of spin relaxation weakens for increasing electron density, leading to constant spin relaxation times for degenerate doping levels. Such high doping densities correspond to very high electronic Fermi temperatures which completely dominate over possible hot-electron heating processes, leading to constant spin relaxation times independent of the excitation density. These results demonstrate the important role played by the optical excitation process and the subsequent cooling dynamics of the optically excited carriers, which can influence the spin dynamics even after the decay of the excited carriers.

ACKNOWLEDGMENTS

We gratefully acknowledge financial support by the German Science Foundation (DFG priority program 1285 "Semiconductor Spintronics" and DFG graduate program GRK 1464 "Micro- and Nanostructures in Optoelectronics and Photonics").

REFERENCES

[1]M. W. Wu, J. H. Jiang, and M. Q. Weng, Phys. Rep. **493**, 61 (2010).
[2]J. H. Jiang and M. W. Wu, Phys. Rev. B **79**, 125206 (2009).
[3]R. I. Dzhioev, K. V. Kavokin, V. L. Korenev, M. V. Lazarev, B. Y. Meltser, M. N. Stepanova, B. P. Zakharchenya, D. Gammon, and D. S. Katzer, Phys. Rev. B **66**, 245204 (2002).
[4]J. H. Buß, J. Rudolph, S. Starosielec, A. Schaefer, F. Semond, Y. Cordier, A. D. Wieck, and D. Hägele, Phys. Rev. B **84**, 153202 (2011).
[5]J. M. Kikkawa and D. D. Awschalom, Phys. Rev. Lett. **80**, 4313 (1998).
[6]R. Bratschitsch, Z. Chen, and S. T. Cundiff, Phys. Status Solidi C **0**, 1506 (2003).
[7]M. Krauß, H. C. Schneider, R. Bratschitsch, Z. Chen, and S. T. Cundiff, Phys. Rev. B **81**, 035213 (2010).
[8]S. A. Crooker, L. Cheng, and D. L. Smith, Phys. Rev. B **79**, 035208 (2009).
[9]L. H. Teng, K. Chen, J. H. Wen, W. Z. Lin, and T. S. Lai, J. Phys. D Appl. Phys. **42**, 135111 (2009).
[10]L. H. Teng, P. Zhang, T. S. Lai, and M. W. Wu, Europhys. Lett. **84**, 27006 (2008).
[11]C. Hautmann, F. Jaworeck, K. Kashani-Shirazi, M.-C. Amann, and M. Betz, Semicond. Sci. Technol. **24**, 025018 (2009).
[12]S. Oertel, J. Hübner, and M. Oestreich, Appl. Phys. Lett. **93**, 132112 (2008).
[13]H. Ma, Z. Jin, G. Ma, W. Liu, and S. Hai Tang, Appl. Phys. Lett. **94**, 241112 (2009).
[14]L. Teng, L. Mu, and X. Wang, AIP Adv. **8**, 105223 (2018).
[15]H. Ma and J. Leng, Phys. Lett. A **377**, 1974 (2013).
[16]H. Ma, Z. Jin, L. Wang, and G. Ma, J. Appl. Phys. **109**, 023105 (2011).
[17]H. Zhao, M. Mower, and G. Vignale, Phys. Rev. B **79**, 115321 (2009).
[18]J. Rudolph, S. Döhrmann, D. Hägele, M. Oestreich, and W. Stolz, Appl. Phys. Lett. **87**, 241117 (2005).
[19]Y. Ohno, R. Terauchi, T. Adachi, F. Matsukura, and H. Ohno, Phys. Rev. Lett. **83**, 4196 (1999); C. Hu, H. Ye, G. Wang, H. Tian, W. Wang, W. Wang, B. Liu, and X. Marie, Nanoscale Res. Lett. **6**, 149 (2011).
[20]K. Shen, Chin. Phys. Lett. **26**, 067201 (2009).
[21]J. H. Jiang and M. W. Wu, J. Phys. D Appl. Phys. **42**, 238001 (2009).
[22]J. H. Jiang and M. W. Wu, Appl. Phys. Lett. **96**, 136101 (2010).
[23]S. Oertel, S. Kunz, D. Schuh, W. Wegscheider, J. Hübner, and M. Oestreich, Europhys. Lett. **96**, 67010 (2011).
[24]P. I. Tamborenea, M. A. Kuroda, and F. L. Bottesi, Phys. Rev. B **68**, 245205 (2003).
[25]M. D. Mower, G. Vignale, and I. V. Tokatly, Phys. Rev. B **83**, 155205 (2011).
[26]R. Klann, O. Brandt, H. Yang, H. T. Grahn, K. Ploog, and A. Trampert, Phys. Rev. B **52**, R11615 (1995).
[27]R. Klann, O. Brandt, H. Yang, H. T. Grahn, and K. H. Ploog, Appl. Phys. Lett. **70**, 1808 (1997).
[28]J. H. Buß, T. Schupp, D. J. As, O. Brandt, D. Hägele, and J. Rudolph, Phys. Rev. B **94**, 235202 (2016).
[29]D. J. As, in *III-Nitride Semiconductor materials: Growth*, edited by M. O. Manasreh and I. T. Ferguson (Taylor and Francis, New York, 2003), Chap. 9; D. J. As, S. Potthast, J. Schörmann, S. F. Li, K. Lischka, H. Nagasawa, and M. Abe, Mater. Sci. Forum **527**, 1489 (2006).
[30]J. H. Buß, J. Rudolph, S. Shvarkov, H. Hardtdegen, A. D. Wieck, and D. Hägele, Appl. Phys. Lett. **102**, 192102 (2013).
[31]M. Muñoz, Y. S. Huang, F. H. Pollak, and H. Yang, J. Appl. Phys. **93**, 2549 (2003).
[32]D. J. As, F. Schmilgus, C. Wang, B. Schöttker, D. Schikora, and K. Lischka, Appl. Phys. Lett. **70**, 1311 (1997).
[33]M. Feneberg, M. Röppischer, C. Cobet, N. Esser, J. Schörmann, T. Schupp, D. J. As, F. Hörich, J. Bläsing, A. Krost, and R. Goldhahn, Phys. Rev. B **85**, 155207 (2012).
[34]O. Brandt, J. Ringling, K. H. Ploog, H.-J. Wünsche, and F. Henneberger, Phys. Rev. B **58**, R15977 (1998).
[35]J. H. Buß, J. Rudolph, F. Natali, F. Semond, and D. Hägele, Phys. Rev. B **81**, 155216 (2010).
[36]D. Hägele, J. Hübner, W. W. Rühle, and M. Oestreich, Physica B **272**, 328 (1999).
[37]M. W. Bayerl, M. S. Brandt, T. Graf, O. Ambacher, J. A. Majewski, M. Stutzmann, D. J. As, and K. Lischka, Phys. Rev. B **63**, 165204 (2001).
[38]J. H. Buß, T. Schupp, D. J. As, D. Hägele, and J. Rudolph, J. Appl. Phys. **118**, 225701 (2015).
[39]A. Schaefer, J. H. Buß, T. Schupp, A. Zado, D. J. As, D. Hägele, and J. Rudolph, J. Appl. Phys. **117**, 093906 (2015).
[40]R. J. Elliott, Phys. Rev. **96**, 266 (1954).
[41]Y. Yafet, Solid State Phys. **14**, 1 (1963).
[42]G. L. Bir, A. G. Aronov, and G. E. Pikus, Sov. Phys. JETP **42**, 705 (1976).
[43]C. Brimont, M. Gallart, O. Crégut, B. Hönerlage, P. Gilliot, D. Lagarde, A. Balocchi, T. Amand, X. Marie, S. Founta, and H. Mariette, J. Appl. Phys. **106**, 053514 (2009).
[44]J. H. Buß, A. Schaefer, T. Schupp, D. J. As, D. Hägele, and J. Rudolph, Appl. Phys. Lett. **105**, 182404 (2014).
[45]J. Rudolph, J. H. Buß, and D. Hägele, Phys. Status Solidi B **251**, 1850 (2014).
[46]K. V. Kavokin, Semicond. Sci. Technol. **23**, 114009 (2008).
[47]M. I. Dyakonov and V. I. Perel, Sov. Phys. Solid State **13**, 3023 (1972).
[48]D. Hägele, S. Döhrmann, J. Rudolph, and M. Oestreich, Adv. Solid State Phys. **45**, 253 (2005).

[49]G. Dresselhaus, Phys. Rev. **100**, 580 (1955).
[50]*Optical Orientation*, edited by F. Meier and B. P. Zakharchenya (North-Holland, Amsterdam, 1984).
[51]S. Krishnamurthy, M. van Schilfgaarde, and N. Newman, Appl. Phys. Lett. **83**, 1761 (2003); Z. G. Yu, S. Krishnamurthy, M. van Schilfgaarde, and N. Newman, Phys. Rev. B **71**, 245312 (2005); A. Tackeuchi, H. Otake, Y. Ogawa, T. Ushiyama, T. Fujita, F. Takano, and H. Akinaga, Appl. Phys. Lett. **88**, 162114 (2006).
[52]J. H. Buß, J. Rudolph, T. Schupp, D. J. As, K. Lischka, and D. Hägele, Appl. Phys. Lett. **97**, 062101 (2010).
[53]M. M. Glazov and E. L. Ivchenko, J. Exp. Theor. Phys. Lett. **75**, 403 (2002).
[54]M. M. Glazov and E. L. Ivchenko, J. Exp. Theor. Phys. **99**, 1279 (2004).
[55]J. Shah, Solid State Electron. **21**, 43 (1978).
[56]S. A. Lyon, J. Lumin. **35**, 121 (1986).
[57]A hyperfine constant $A_{\mathrm{Ga}} = 42\,\mu$eV averaged over the ^{69} Ga and ^{71} Ga isotopes is used, the effect of the N nuclei is neglected as compared to the Ga nuclei and the number of interacting nuclei N_L is approximated by the ratio of the localization volume V_L to the unit cell volume v_0 of β-GaN. The localization volume is approximated by $V_L = 4/3\pi\tilde{a}_B^3$ with the modified Bohr radius $\tilde{a}_B = 1.5\varepsilon/(m^*/m_0)a_H$, where a_H is the Bohr radius of an H atom.
[58]A spin-splitting constant of 2.5 eVÅ^3 and a typical dislocation density of 5×10^9 cm^{-2} was used for the estimate.
[59]R. Ulbrich, Phys. Rev. B **8**, 5719 (1973).
[60]P. Lugli, P. Bordone, L. Reggiani, M. Rieger, P. Kocevar, and S. M. Goodnick, Phys. Rev. B **39**, 7852 (1989).
[61]X. Q. Zhou, H. M. van Driel, W. W. Rühle, and K. Ploog, Phys. Rev. B **46**, 16148 (1992).
[62]S. K. Pugh, D. J. Dugdale, S. Brand, and R. A. Abram, Semicond. Sci. Technol. **14**, 23 (1999).
[63]H. Siegle, L. Eckey, A. Hoffmann, C. Thomsen, B. K. Meyer, D. Schikora, M. Hankeln, and K. Lischka, Solid State Commun. **96**, 943 (1995).
[64]D. J. As, D. Schikora, A. Greiner, M. Lübbers, J. Mimkes, and K. Lischka, Phys. Rev. B **54**, 11118 (1996).
[65]K. Shimada, T. Sota, and K. Suzuki, J. Appl. Phys. **84**, 4951 (1998).
[66]V. Bougrov, M. Levinshtein, S. Rumyantsev, and A. Zubrilov, in *Properties of Advanced Semiconductor Materials*, edited by M. E. Levinshtein, S. L. Rumyantsev, and M. S. Shur (Wiley, New York, 2001), Chap. 1.
[67]K. Kim, W. R. L. Lambrecht, and B. Segall, Phys. Rev. B **53**, 16310 (1996).
[68]C. Weisbuch, Solid State Electron. **21**, 179 (1978).
[69]D. M. Eagles, J. Phys. Chem. Solids **16**, 76 (1960).